Electronic Supplementary Information (ESI)

Influence of local strain caused by cycloaddition on the band gap control of functionalized single-walled carbon nanotubes

Yutaka Maeda,[*a] Kiyonori Kuroda,[a] Haruto Tambo,[a] Hiyori Murakoshi,[a] Yui Konno,[a] Michio Yamada[a], Pei Zhao,[b] Xiang Zhao,[c] Shigeru Nagase,[d] Masahiro Ehara[*b]

[a]Department of Chemistry, Tokyo Gakugei University, Tokyo 184-8501, Japan

[b]Research Center for Computational Science, Institute for Molecular Science, Okazaki, 444-8585, Japan

[c]Institute for Chemical Physics & Department of Chemistry, School of Science, State Key Laboratory of Electrical Insulation and Power Equipment, Xi'an Jiaotong University, Xi'an 710049, China

[d]Fukui Institute for Fundamental Chemistry (FIFC), Kyoto University, Sakyou-ku, Kyoto 606-8103, Japan

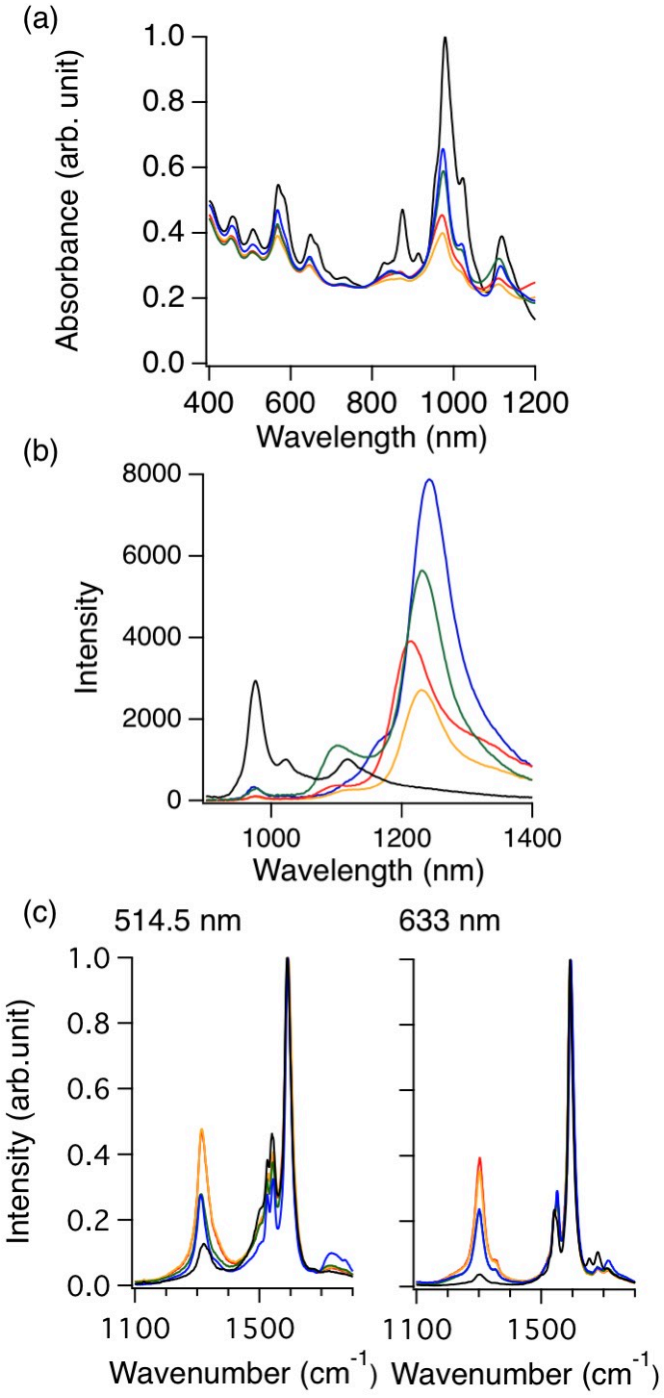

Fig. S1 (a) Absorption spectra normalized by the local minimum near 775 nm, (b) PL spectra (567 nm excitation), and (c) Raman spectra of SWNTs (Black) and **2a** (Red), **2b** (Yellow), **2c** (Green), and **2d** (Blue) dispersed in D_2O containing 1 wt% SDBS.

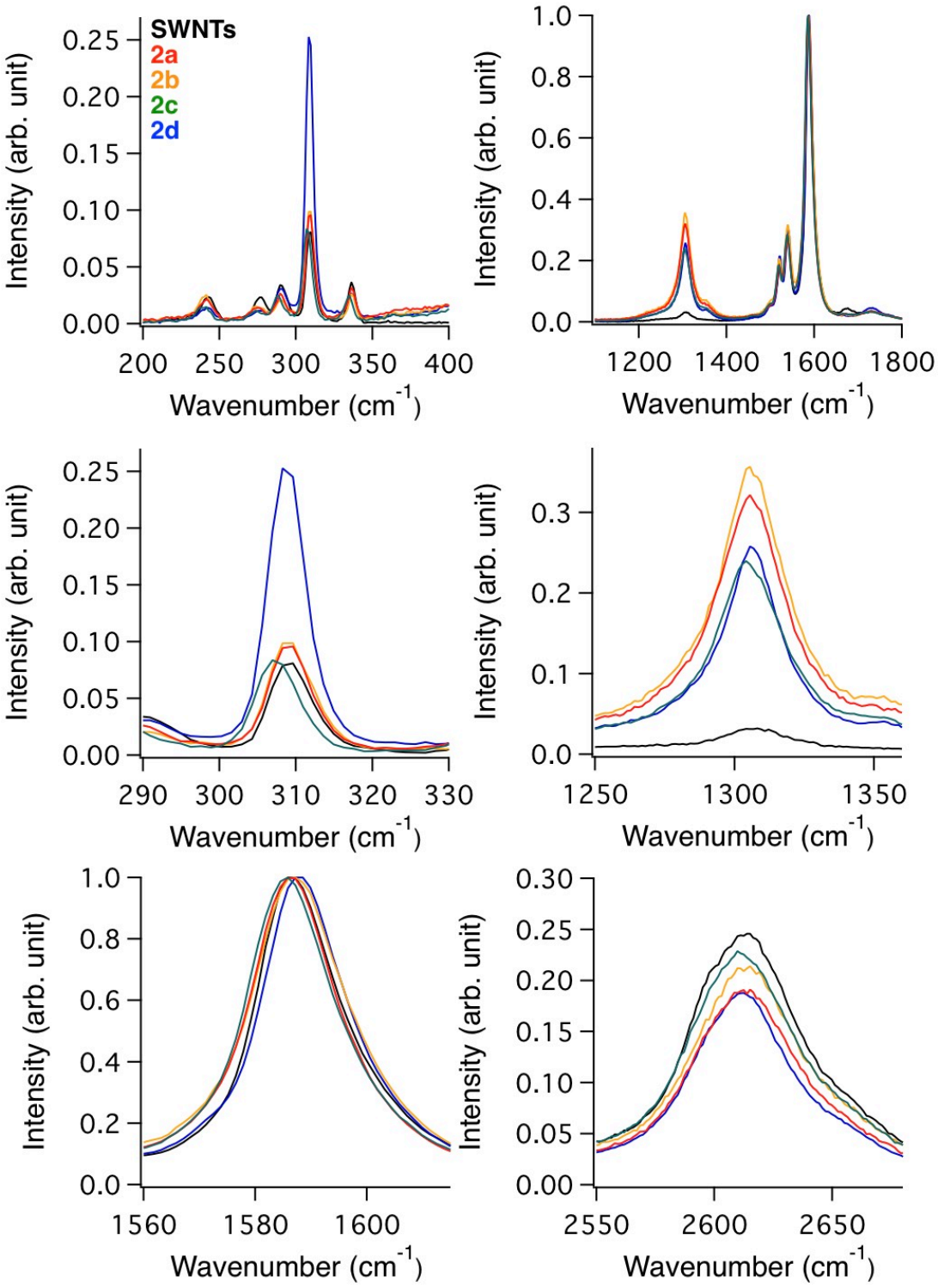

Fig. S2 Raman spectra of SWNTs and **2a**-**2d** (561 nm excitation).

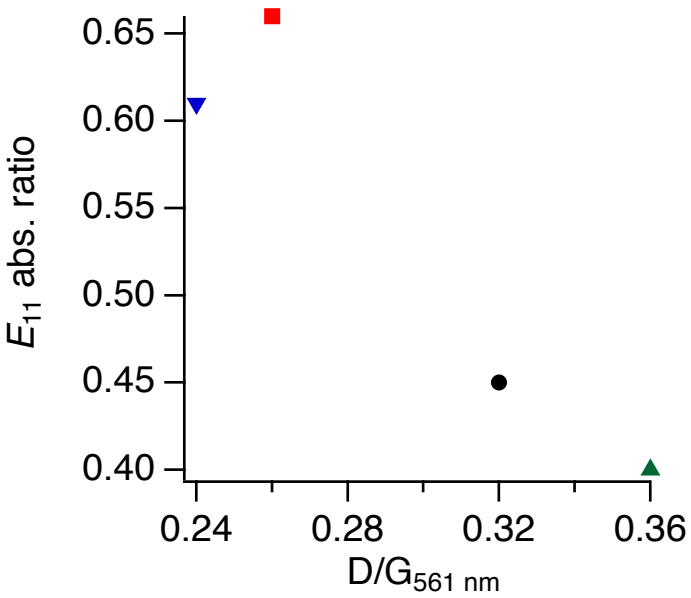

Fig. S3 E_{11} abs. ratio as a function of D/G (561 nm excitation).

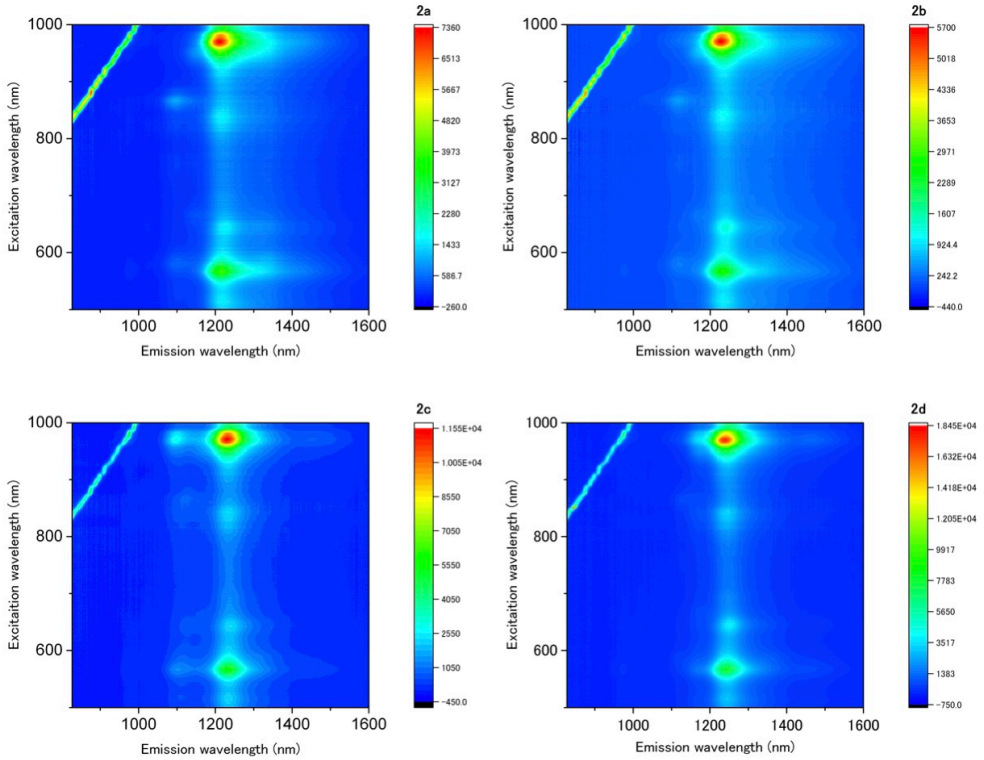

Fig. S4 Contour plots of PL intensity versus excitation and emission wavelengths of **2** dispersed in D_2O containing 1 wt% SDBS.

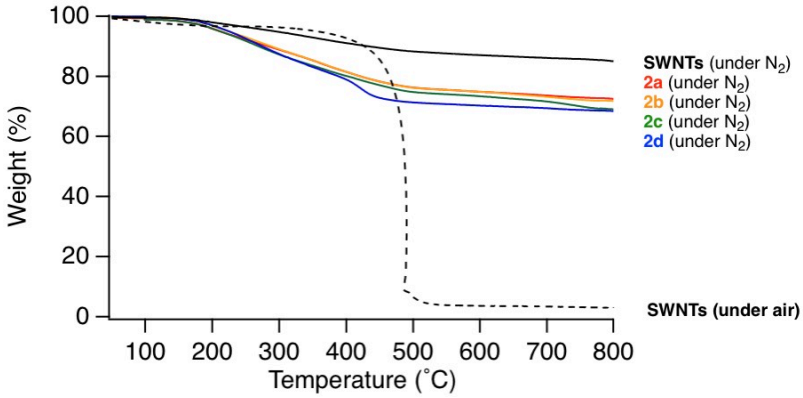

Fig. S5 TG curve of SWNTs and **2a-2d**. Heating rate:10˚C/min. Gas flow rate: 50 mL/min.

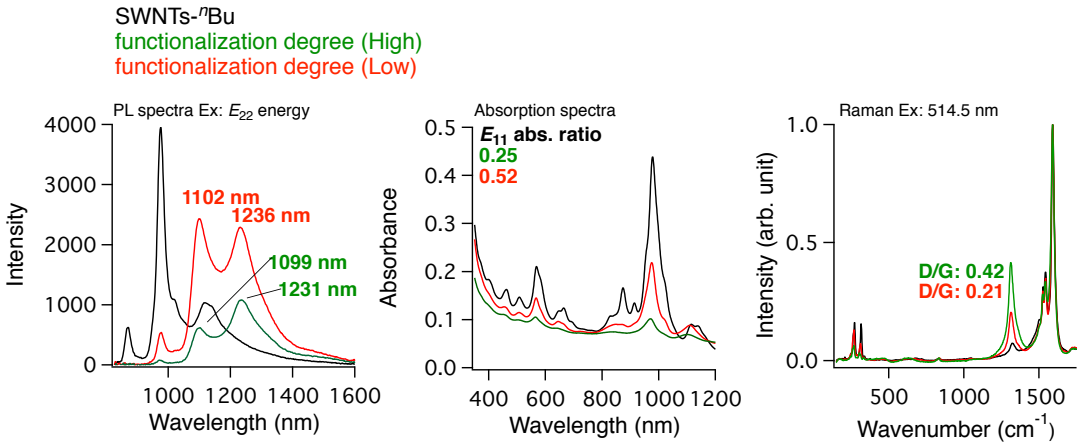

Fig. S6 PL, absorption, and Raman spectra of butylated SWNTs having different functionalization degree.[1]

[1]Y. Maeda, Y. Takehana, J.-S. Dang, M. Suzuki, M. Yamada, S. Nagase, *Chem. Eur. J.* 2017, **23**, 1789-1794.

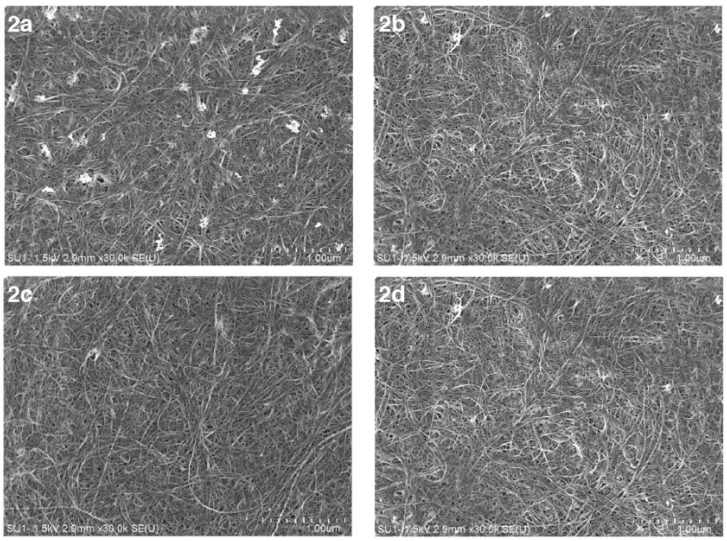

Fig. S7 SEM images of **2a-2d.**

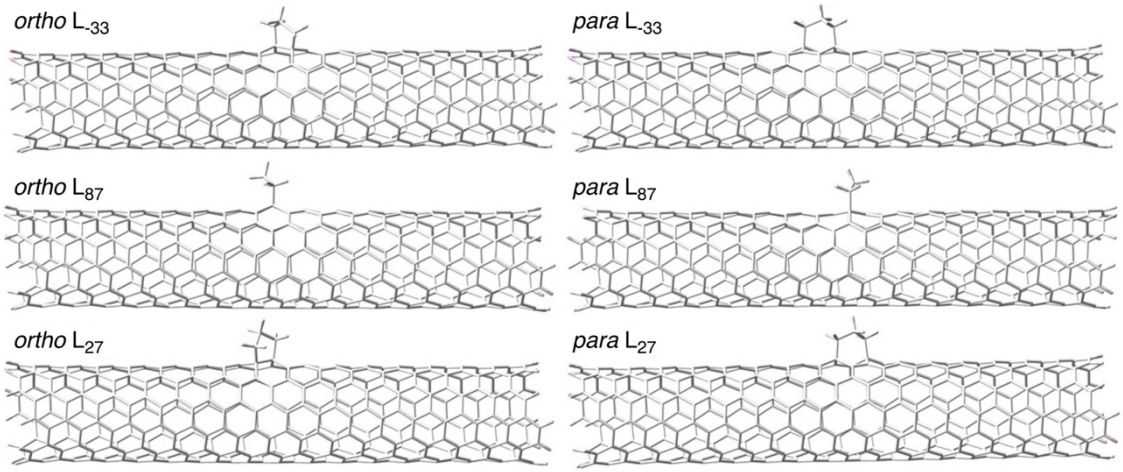

Fig. S8 The optimized structures of six adducts for SWNT-(C_3H_6).

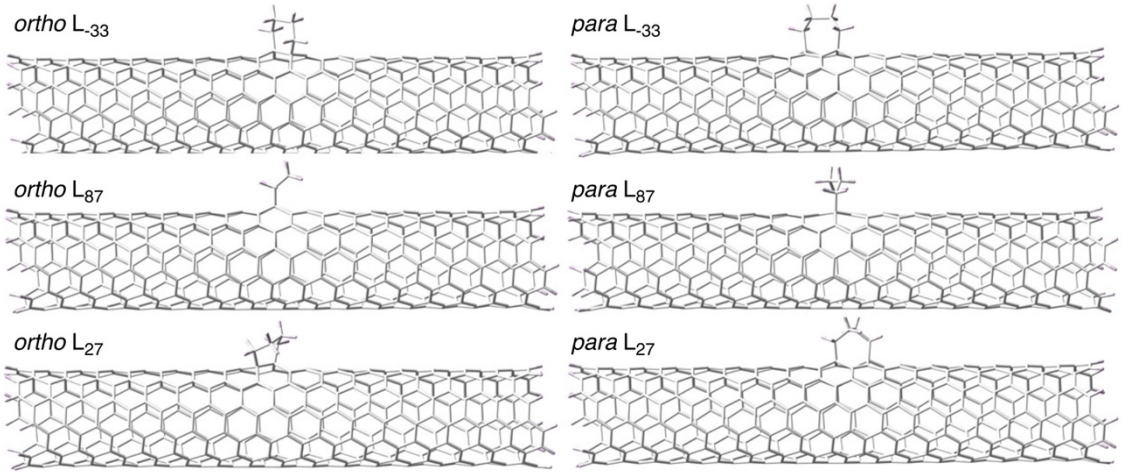

Fig. S9 The optimized structures of six adducts for SWNT-(C_4H_8).

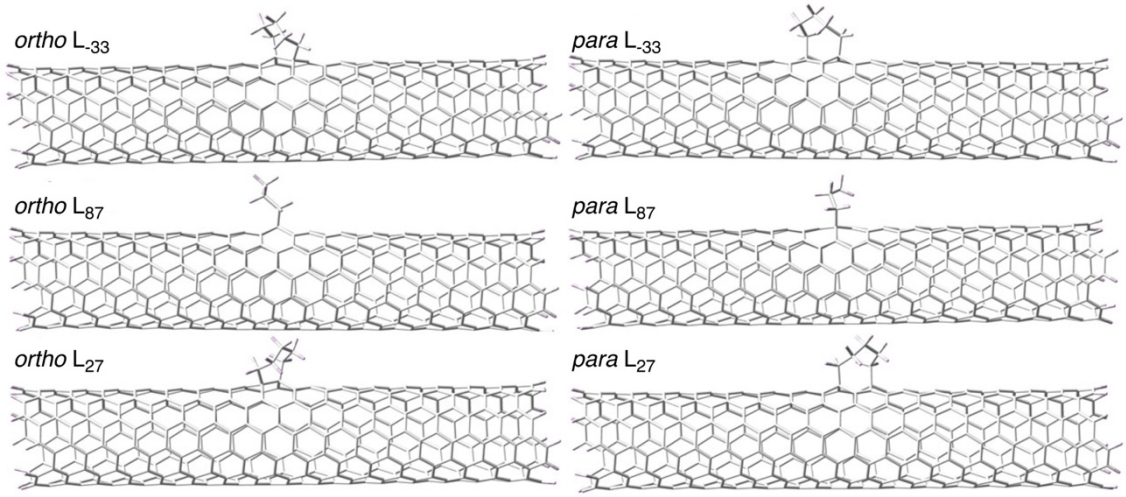

Fig. S10 The optimized structures of six adducts for SWNT-(C_5H_{10}).

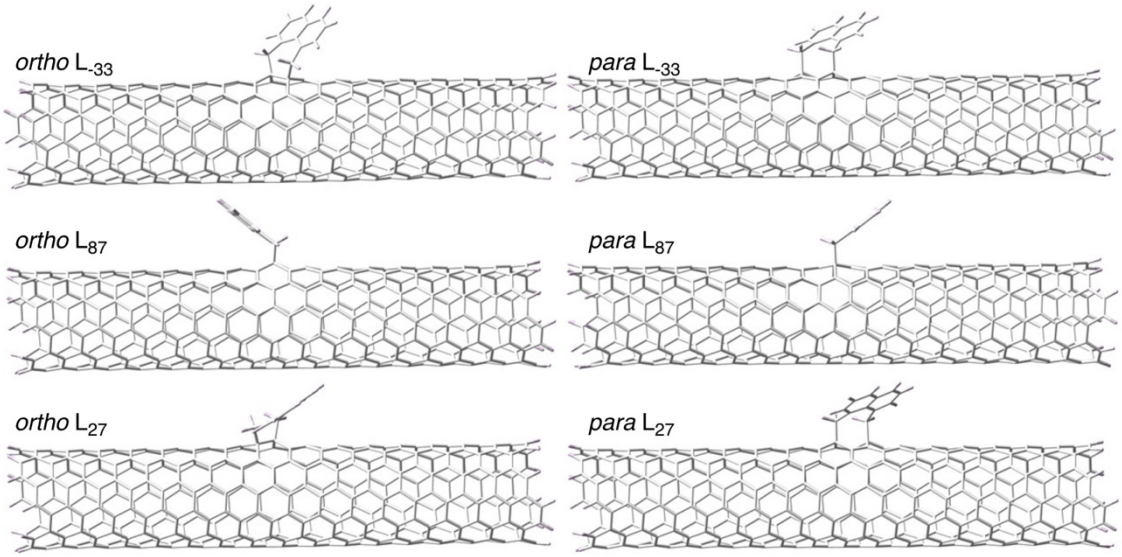

Fig. S11 The optimized structures of six adducts for SWNT-($C_{12}H_{10}$).

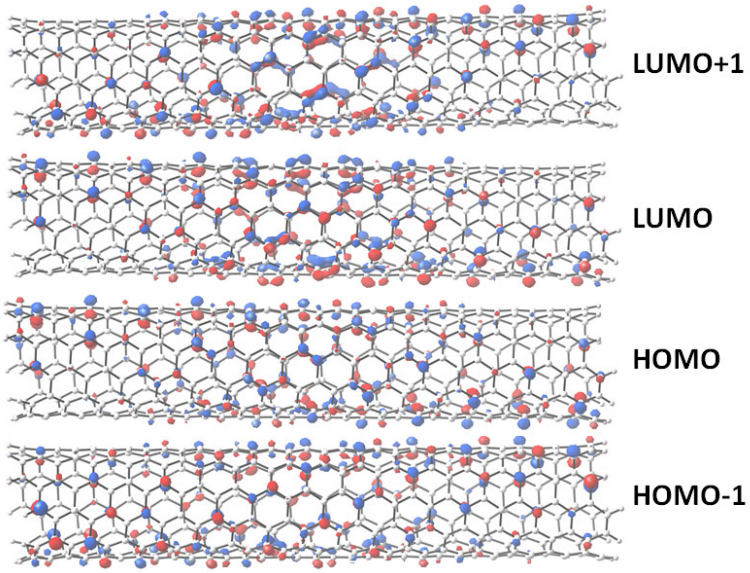

Fig. S12 Frontier molecular orbital diagrams of the pristine (6,5) SWNT at the level of B3LYP/6-31G* (isovalue=0.02).

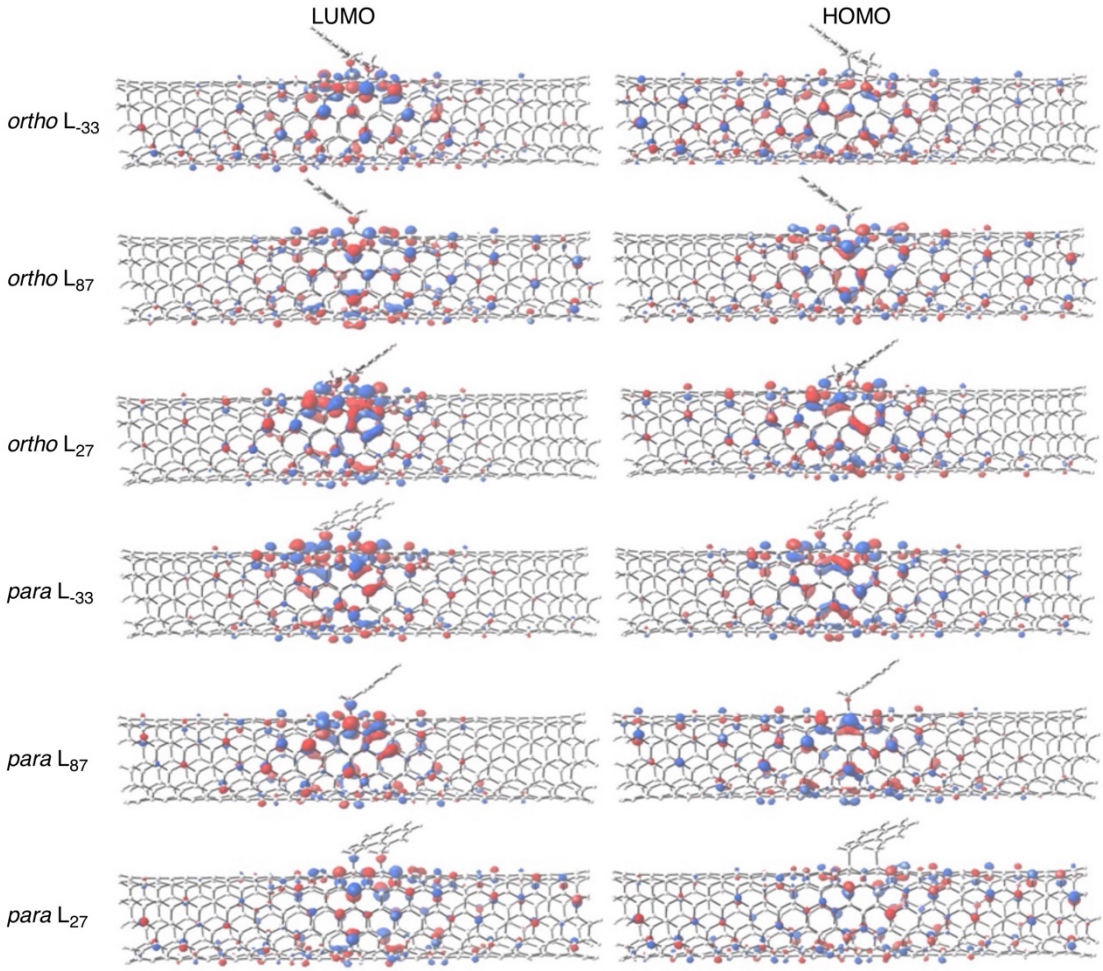

Fig. S13 Frontier molecular orbital diagrams of ortho and para adducts for SWNT-($C_{12}H_{10}$) (B3LYP/6-31G*, isovalue=0.02).

Table S1. Relative energies (in kcal/mol) of functionalized (6,5) SWNTs calculated by DFT with B3LYP/6-31G*.

Carbon position	SWNT-(C_3H_6)	SWNT-(C_4H_8)	SWNT-(C_5H_{10})	SWNT-($C_{12}H_{10}$)
ortho L_{-33}	0	0	0	0
ortho L_{27}	1.9	3.7	2.4	2.4
ortho L_{87}	4.6	7.9	5.8	5.8
para L_{27}	9.6	6.4	11.3	13.2
para L_{-33}	15.8	11.7	14.5	17.5
para L_{87}	46.5	18.2	5.6	39.0

Table S2. Bond angles of different addition sites in pristine and functionalized (6,5) SWNTs at the level of B3LYP/6-31G*.

Addition		SWNT			SWNT-(C_3H_6)			SWNT-(C_4H_8)			SWNT-(C_5H_{10})			SWNT-($C_{12}H_{10}$)		
positions		a_1	a_2	a_3	a_1	a_2	a_3	a_1	a_2	a_3	a_1	a_2	a_3	a_1	a_2	a_3
ortho L_{-33}	*a*	119.1	119.5	118.7	107.6	111.8	116.0	106.4	111.1	114.4	105.6	111.9	113.7	106.3	112.0	114.1
	b	119.1	119.5	118.7	107.2	111.4	115.1	106.4	111.1	114.4	106.1	111.7	114.2	106.5	111.9	114.6
ortho L_{87}	*a*	119.5	118.7	119.1	113.4	112.6	112.2	112.7	112.1	112.0	112.1	111.6	112.0	112.5	111.9	112.3
	d	119.5	118.7	119.1	113.4	112.3	112.4	112.7	112.1	112.2	112.1	112.0	111.7	112.6	112.2	111.9
ortho L_{27}	*a*	118.7	119.1	119.5	106.1	115.4	111.8	105.4	115.0	112.5	104.4	114.5	112.1	105.1	114.5	112.1
	f	118.7	119.1	119.5	106.5	116.2	112.2	105.5	114.5	112.1	105.0	114.7	111.7	105.4	115.0	112.1
para L_{-33}	*a*	119.5	118.7	119.1	112.0	108.2	108.6	112.4	108.2	108.0	112.2	107.2	107.5	112.4	108.3	108.2
	e	119.5	118.7	119.1	112.1	108.2	108.8	112.4	108.2	108.0	112.6	108.0	107.7	112.3	107.9	108.1
para L_{87}	*a*	118.7	119.1	119.5	107.1	107.6	114.3	107.6	108.3	112.6	107.7	108.7	111.7	107.5	107.6	113.0
	g	118.7	119.1	119.5	107.0	107.7	114.4	107.6	108.3	112.6	108.0	108.4	111.7	107.0	108.1	113.0
para L_{27}	*a*	119.1	119.5	118.7	109.0	112.3	107.8	108.8	112.8	107.4	108.1	112.2	106.6	108.7	112.4	107.2
	c	119.1	119.5	118.7	109.1	112.2	107.6	108.8	112.8	107.3	108.7	112.7	106.8	109.0	112.6	107.3

Table S3. Sum of bond angles at the addition sites in pristine and functionalized (6,5) SWNTs at the level of B3LYP/6-31G*.

Addition position		SWNTs	SWNT-(C_3H_6)	SWNT-(C_4H_8)	SWNT-(C_5H_{10})	SWNT-($C_{12}H_{10}$)
ortho L_{-33}	*a*	357.3	335.4	331.9	331.2	332.4
	b	357.3	333.7	331.9	332.0	333.0
ortho L_{87}	*a*	357.3	338.2	336.8	335.7	336.7
	d	357.3	338.1	337.0	335.8	336.7
ortho L_{27}	*a*	357.3	333.3	332.9	331.0	331.7
	f	357.3	334.9	332.1	331.4	332.5

Table S4. Calculated absorption and emission wavelengths (in nm) of functionalized (6,5) SWNTs (*ortho* L_{-33}) using TD-DFT with B3LYP/3-21G.

	SWNT	SWNT-(C_3H_6)	SWNT-(C_4H_8)	SWNT-(C_5H_{10})	SWNT-($C_{12}H_{10}$)	SWNT-$(CH_3)_2$[a]
Absorption wavelength (calcd.)	790	880	885	892	896	889
Emission wavelength (calcd.)	806	922	927	932	936	930
Stokes shift	16	42	42	40	40	41

[a] The structure of SWNT in SWNT-$(CH_3)_2$ was taken as the same as that in SWNT-($C_{12}H_{10}$).

Table S5. HOMO-LUMO gaps (in eV) of (6.5)-SWNT and functionalized (6,5) SWNTs (B3LYP/6-31G*).

Addition position	SWNT	SWNT-(C_3H_6)	SWNT-(C_4H_8)	SWNT-(C_5H_{10})	SWNT-($C_{12}H_{10}$)
ortho L_{-33}	1.69	1.62	1.61	1.60	1.60
ortho L_{27}	1.69	1.30	1.28	1.28	1.27
ortho L_{87}	1.69	1.55	1.53	1.53	1.53
para L_{27}	1.69	1.66	1.67	1.67	1.66
para L_{-33}	1.69	1.25	1.27	1.26	1.26
para L_{87}	1.69	1.41	1.43	1.43	1.42

Table S6. Total energies (in a.u.) of functionalized (6,5) SWNTs calculated by DFT with B3LYP/6-31G*.

Addition position	SWNT-(C_3H_6)	SWNT-(C_4H_8)	SWNT-(C_5H_{10})	SWNT-($C_{12}H_{10}$)
ortho L_{-33}	-14003.7374286	-14043.0454506	-14082.3472172	-14349.1068842
ortho L_{27}	-14003.7343939	-14043.0395043	-14082.3433409	-14349.1030330
ortho L_{87}	-14003.7301413	-14043.0329049	-14082.3379451	-14349.0977008
para L_{27}	-14003.7221869	-14043.0351775	-14082.3291672	-14349.0859153
para L_{-33}	-14003.7123257	-14043.0268116	-14082.3240413	-14349.0790522
para L_{87}	-14003.6632968	-14043.0164373	-14082.3383659	-14349.0446623

Table S7. Calculated absorption wavelength (in nm) of SWNT-($C_3H_6Br)_2$, SWNT-($C_4H_8Br)_2$, H-SWNT-(C_3H_6Br), and H-SWNT-(C_4H_8Br) at the level of B3LYP/3-21G.

Addition position	Functionalized SWNTs	Absorption wavelength	Oscillator strength
para L_{87}	SWNT-($C_3H_6Br)_2$	1005	0.8951
	SWNT-($C_4H_6Br)_2$	1003	0.9049
ortho L_{-33}	H-SWNT-C_3H_6Br	890	0.5075
	H-SWNT-C_4H_6Br	889	0.5123

Table S8. Weight loss, weight ratio of addenda to SWNTs in functionalized SWNTs, and functional group coverage (FGC).

	2a	**2b**	**2c**	**2d**
Weight ratio of addenda to SWNTs[1,2]	15.1 : 84.9	16.0 : 84.0	19.3 : 80.7	19.9 : 80.1
FGC[3] (number of C / one substituent)	19.7	24.6	24.5	51.5

1 Ratio of SWNTs and catalyst (wt%) was 97.0 : 3.0 estimated by TGA under air.

2 wt% of addenda was corrected by wt loss of SWNTs under the same condition.

3 F. G. Brunetti, M. A. Herrero, J. D. M. Muñoz, A. Díaz-Ortiz, J. Alfonsi, M. Meneghetti, Prato, E. J. Vázquez, E. *J. Am. Chem. Soc.* 2008, **130**, 8094-8100.